Article

Not peer-reviewed version

Effect of Ceria doping on the Mechanical Properties and Phase Stability of Partially Samaria-Stabilized Zirconia Crystals

Mikhail Borik , Artem Chislov , Alexej Kulebyakin , Elena Lomonova , Filipp Milovich , Valentina Myzina , Vladimir Pankratov , Alexandr Poselennov , Polina Ryabochkina , Nataliya Tabachkova * , Nataliya Sidorova , Dmitriy Zakharov , Dmitriy Kiselev

Posted Date: 12 July 2024

doi: 10.20944/preprints202407.1010.v1

Keywords: partially stabilized zirconia; skull melting; solid solutions; mechanical properties; ZrO2

Article

Effect of Ceria doping on the Mechanical Properties and Phase Stability of Partially Samaria-Stabilized Zirconia Crystals

Mikhail Borik [1], Artem Chislov [1,2], Alexej Kulebyakin [1], Elena Lomonova [1], Filipp Milovich [2,3], Valentina Myzina [1], Vladimir Pankratov [4], Alexandr Poselennov [2], Polina Ryabochkina [5], Nataliya Sidorova [5] and Nataliya Tabachkova [1,2,*], Dmitriy Zakharov [1,2], Dmitriy Kiselev [2]

[1] Prokhorov General Physics Institute of the Russian Academy of Sciences, 38 Vavilov Str., 119991 Moscow, Russia; borik@lst.gpi.ru (M.B.); chislov.artem@bk.ru (A.C.); kulebyakin@lst.gpi.ru (A.K.); lomonova@lst.gpi.ru (E.L.); vamyzina@lst.gpi.ru (V.M.); ntabachkova@gmail.com (N.T.)

[2] Department of Materials Science of Semiconductors and Dielectrics, National University of Science and Technology (MISIS), 4 Leninskiy prospekt, 119049 Moscow, Russia, poselennovs@gmail.com (A.P), deniszakharovm@mail.ru (D.Z), dm.kiselev@gmail.com (D.K)

[3] Department of Materials Science, Moscow Polytechnic University, Bolshaya Semyonovskaya Street, 38, philippmilovich@gmail.com;

[4] Institute of Solid State Physics, University of Latvia, 8 Kengaraga Iela, Riga 1063, LV, Latvia; vladimirs.pankratovs@cfi.lu.lv (V.P)

[5] Institute of High Technologies and New Materials, Ogarev Mordovia State University, 68 Bolshevistskaya Str., 430005 Saransk, Republic of Mordovia, Russia; ryabochkina@freemail.mrsu.ru (P.R.); ya.natalka2112@yandex.ru (N.S.)

* Correspondence: ntabachkova@gmail.com Tel.: +7-(916)-647-19-54

Abstract: The effect of ceria doping of $(ZrO_2)_{1-x}(Sm_2O_3)_x$ crystals on their phase composition, microhardness and fracture toughness has been studied. The $(ZrO_2)_{0.995-x}(Sm_2O_3)_x(CeO_2)_{0.005}$ crystals (where x = 0.032, 0.037 and 0.04) have been grown using directional melt crystallization in cold skull. The phase composition and structure of the crystals have been studied using X-ray diffraction, TEM and Raman spectroscopy. The mechanical properties such as microhardness and fracture toughness have been studied using Vickers indentation. It has been shown that the $(ZrO_2)_{0.995-x}(Sm_2O_3)_x(CeO_2)_{0.005}$ solid solution crystals contain both Ce^{4+} and Ce^{3+} ions. Phase analysis data suggest that CeO_2 doping increases the tetragonality degree of the transformable t phase and reduces the tetragonality degree of the non-transformable t' phase as compared to the $(ZrO2)_{1-x}(Sm2O3)x$ crystals. As a result, the t→m phase transition triggered by the indentation-induced stress in the CeO_2 doped crystals is more intense and covers greater regions. CeO2 doping of the solid solutions increases the fracture toughness of all the crystals studied whereas the microhardness of the crystals changes but slightly. CeO_2 doping of the $(ZrO_2)_{1-x}(Sm_2O_3)_x$ solid solutions in the experimental concentration range does not improve the high-temperature phase stability of the crystals and does not prevent high-temperature degradation of their fracture toughness.

Keywords: partially stabilized zirconia; skull melting; solid solutions; mechanical properties; ZrO_2

1. Introduction

Partially stabilized zirconia based materials possess good mechanical properties providing for their wide application range, including construction ceramics, wear-resistant bearings, heat protective coatings, oxygen conducting solid state electrolytes, biomedical devices etc. [1–5].

The high strength of the abovementioned materials is primarily determined by the transformation strengthening mechanism [1,2,6]. Strengthening takes place as a result of a phase transition from the metastable tetragonal phase to the stable monoclinic one the lattice parameters of which are greater than those of the tetragonal phase. The phase composition of zirconia based solid

 doi:10.20944/preprints202407.1010.v1

solutions depends on the type and concentration of stabilizing oxides [7–9]. The most widely used stabilizing oxides are yttria and ceria. ZrO_2 based solid solutions partially stabilized with CeO_2 are of great interest due to their high fracture toughness [2,10–14]. However, the strength parameters of those materials such as microhardness, Young's modulus and flexure strength are inferior to those of yttria-stabilized zirconia based materials.

Apart from yttria, almost all trivalent rare-earth element cations form zirconia based solid solutions. Earlier data [15] suggest that solid solutions stabilized with large-radius trivalent cations exhibit a tendency to more efficient phase separation. In other words, the greater the radius of the trivalent cation, the closer the tetragonality degrees of the metastable (t) and (t') phases to those of the equilibrium t and c phases which are 1.022 [16] and 1.0, respectively. This is in agreement with earlier data [17] showing that the width of the (c+t) two-phase region depends on the cation type, i.e., it increases with cation radius. The proximity of the metastable t phase composition to the t/(c+t) phase boundary favors the stress-induced t→m phase transition and hence increases the transformability of the material. Comparison between the mechanical properties of the crystals depending on the ionic radius of trivalent cation in the series RY^{3+} = 1.019 Å < RGd^{3+} = 1.053 Å < RSm^{3+} = 1.074 Å showed that the fracture toughness of the $(ZrO_2)_{1-x}(R_2O_3)_x$ tetragonal crystals, where R = Y, Gd, Sm, increases with the ionic radius of the trivalent cation [15]. However, the fracture toughness of the synthesized partially stabilized zirconia decreases significantly if the material contains the monoclinic phase. Along with the good mechanical parameters, of special importance is the long-term stability of their parameters under cycled loads and at elevated temperatures and humidity [18–21]. Optimization of the mechanical properties of the materials and increasing their stability are achieved through co-doping with several oxides. There are a number of works dealing with yttria and ceria co-doping of zirconia and study of their parameters depending on the composition, grain structure and synthesis conditions [8,9,22]. However, there are but a few publications on co-doping with ceria and other rare-earth element oxides. YSZ co-doping with ceria and neodymia delivered good mechanical properties and furthermore provided for their preservation upon heat treatment [23]. One can expect that co-doping of ZrO_2 based solid solutions with ceria and rare-earth element oxides having greater cation radius than Y^{3+} will produce materials combining high strength and fracture toughness.

The aim of this work is to study the effect of ceria doping of $(ZrO_2)_{1-x}(Sm_2O_3)_x$ crystals on their phase composition, microhardness and fracture toughness. The experimental results were compared with earlier data on $(ZrO_2)_{1-x}(Sm_2O_3)_x$ crystals [24].

2. Materials and Methods

The test crystals were grown using directional melt crystallization in a 100 mm diam. water-cooled crucible with direct inductive heating. The power source was a 63 kW 5.28 MHz high-frequency generator. The raw powders (at least 99.99% purity) were mechanically mixed and loaded into the crucible. The charge weight was 4.5–5 kg. Melting was initiated using metallic zirconium. The melt was crystallized by moving the crucible out of the heating zone at a 10 mmph speed. The cross-sections and lengths of the crystals were 10 to 20 mm and 30 to 40 mm, respectively.

The phase composition of the crystals was studied using X-ray diffraction and Raman spectroscopy on a BrukerD8 diffractometer and a RenishawinVia microscope/spectrometer, respectively. Plates for the tests were cut out from the middle parts of the crystals. The crystals grown by directional melt crystallization in a cold skull had no preferential growth orientations. Therefore, the actual crystal orientations were identified by X-ray diffraction and test plates were then cut out perpendicular to the <100> direction.

The structure of the crystals was studied using transmission electron microscopy (TEM) under a JEM-2100 microscope at a 200 kV acceleration voltage. The TEM specimens were prepared by ion beam thinning on a PIPSII instrument.

The microhardness and cracking resistance of the crystals were compared by indentation in the {100} plane for different specimen rotation angles in the specimen plane. The tests were conducted with a DM 8 B AUTO microhardness tester (Vicker's indenter, maximum load 20 N) and a Wolpert

 doi:10.20944/preprints202407.1010.v1

Hardness Tester 930 with a minimum load of 50 N. The as-cut specimens were chemomechanically polished for damaged surface layer removal. The as-treated surface had no micro- or nanocracks and was leveled and smooth.

The cracking resistance (K1c) was calculated using Niihara's formula for the Palmqvist Crack system [25–27]

$$K_{1c} = 0{,}035(L/a)^{-1/2}(CE/H)^{2/5}\,Ha^{1/2}C^{-1} \quad (1)$$

where K1c is the stress intensity coefficient (MPa·m1/2); L is the radial crack length (m); a is the indentation half-width (m); C is the constraint factor (=3); E is Young's modulus (Pa); H is the microhardness (Pa).

For K1c calculation, radial cracks around the indentation were taken the length of which met the criterion ($0.25 \le l/a \le 2.5$) for Palmqvist craks.

3. Results and Discussion

The test crystals had the compositions $(ZrO_2)_{1-x}(Sm_2O_3)_x$ (where x= 0.032, 0.037 and 0.04) and were additionally doped with 0.5 mol.% CeO_2. Hereinafter the crystals compositions will be denoted as 3.2Sm0.5CeSZ, 3.7Sm0.5CeSZ and 4.0Sm0.5CeSZ, respectively. The 0.5 mol.% ceria concentration was chosen based on the following reasons. On the one hand, cerium containing ceramics having high fracture toughness typically have higher ceria concentrations. On the other hand, directional melt crystallization of high-ceria crystals causes ceria displacement from the crystallization front and eventually hinders the growth of homogeneous single crystals.

The as-grown $(ZrO_2)_{0.995-x}(Sm_2O_3)_x(CeO_2)_{0.005}$ single crystals had orange color due to Ce^{3+} ions, this color changing after air annealing. The orange/red color is caused by the wide absorption band near 460 nm originating from the 4f→5d transition of Ce^{3+} ions [28]. The presence of Ce^{3+} ions in the crystals is further confirmed by on the X-ray adsorption near-edge structure data (XANES). Figure 1 shows the XANES spectrum of the 4.0Sm0.5CeSZ crystal exhibiting two clear absorption bands at 5732 and 5738 eV corresponding to the Ce4+ ions and a broadened absorption band at 5727 eV corresponding to the Ce^{3+} ions [29]. The data suggest that the $(ZrO_2)_{0.995-x}(Sm_2O_3)_x(CeO_2)_{0.005}$ crystals contain both Ce^{4+} and Ce^{3+} ions.

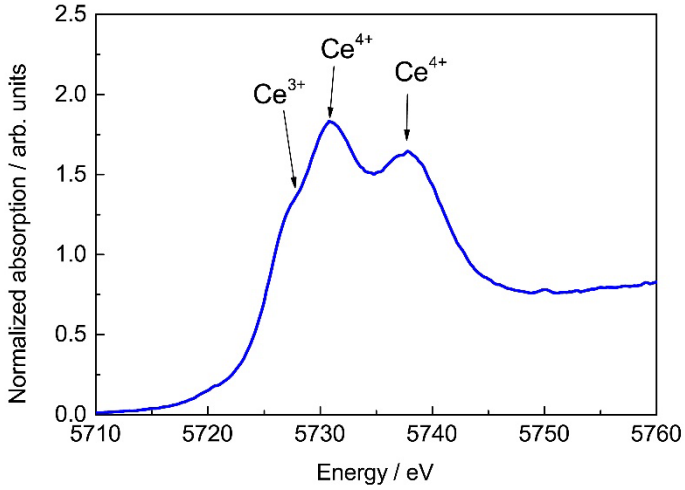

Figure 1. Ce ion XANES spectrum of 4.0Sm0.5CeSZ crystal.

X-ray phase data show that the 3.2Sm0.5CeSZ crystals contain a mixture of the monoclinic (m) and tetragonal (t) phases of zirconia. It should be noted that those crystals were visibly inhomogeneous in the bulk and had a few cracks. Those macrodefects are probably caused by polymorphic transitions occurring during crystal cooling that are accompanied by volumetric changes. This phase composition was also typical of the 3.2SmSZ crystals that did not contain ceria [24]. Thus, ceria doping of crystals containing 3.2 mol.% stabilizing oxide did not stabilize the tetragonal phase in the whole bulk of the crystals. Other crystals contained only the tetragonal

 doi:10.20944/preprints202407.1010.v1

modifications of zirconia. Some structural parameters of the tetragonal crystals are presented in Table 1. By way of comparison, Table 1 also shows earlier data for $(ZrO_2)_{1-x}(Sm_2O_3)_x$ crystals [15].

Table 1. Phase composition, lattice parameters and tetragonality degree of $(ZrO_2)_{0.995-x}(Sm_2O_3)_x(CeO_2)_{0.005}$ and $(ZrO_2)_{1-x}(Sm_2O_3)_x$ crystals.

Specimen	Phase	Content, wt.%	Lattice Parameters, Å	c/√2a
3.7SmSZ [24]	t	85 ± 5	a = 3.6062(2) c = 5.1866(2)	1.0170
	t′	15 ± 5	a = 3.6426(5) c = 5.1695(2)	1.0035
3.7Sm0.5CeSZ	t	90 ± 5	a = 3.6062(2) c = 5.1886(2)	1.0174
	t′	10 ± 5	a = 3.6426(5) c = 5.1682(2)	1.0032
4.0SmSZ[24]	t	75 ± 5	a = 3.6063(2); c = 5.1854(2)	1.0167
	t′	25 ± 5	a = 3.6429(5); c = 5.1692(2)	1.0034
4.0Sm0.5CeSZ	t	85 ± 5	a = 3.6063(1) c = 5.1877(2)	1.0172
	t′	15 ± 5	a = 3.6427(5) c = 5.1685(2)	1.0033

Analysis of the data in Table 1 shows that doping with 0.5 mol.% CeO_2 affects the lattice parameter c of the tetragonal phase the most effectively. For example, the lattice parameter c of the t phase grows from 5.1866 to 5.1886 Å for the 3.7SmSZ crystals and from 5.1854 to 5.1877 Å for the 4.0SmSZ ones. The lattice parameter c of the t′ phase decreases from 5.1695 to 5.1682Å for 3.7SmSZ and from 5.1692 to 5.1685 Å for 4.0SmSZ. Thus, CeO_2 doping increases the tetragonality degree of the transformable t phase and reduces the tetragonality of the non-transformable t′ phase. The tetragonality degree of zirconia based tetragonal solid solutions is known to be directly related to the content of the stabilizing oxide [30]. The observed changes in the tetragonality degree of the t and t′ phases suggest that CeO_2 doping causes a more efficient phase separation in the (c + t) two-phase region. The transformable t phase becomes more transformable as its composition approaches the t/(c + t) phase boundary, whereas the composition of the non-transformable t′ phase shifts toward the (c + t)/c phase boundary. Similar results were obtained for the Yb_2O_3—Nd_2O_3—ZrO_2 ceramics (1Yb–2Nd–TZP) which also exhibited phase separation accompanied by a decrease in the concentration of stabilizing oxides in the tetragonal grains which made the materials more transformable [31].

TEM study did not reveal differences between the structures of the $(ZrO_2)_{0.995-x}(Sm_2O_3)_x(CeO_2)_{0.005}$ and $(ZrO_2)_{1-x}(Sm_2O_3)_x$ crystals. Figure 2 shows a TEM image of the 3.7Sm0.5CeSZ crystal.

 doi:10.20944/preprints202407.1010.v1

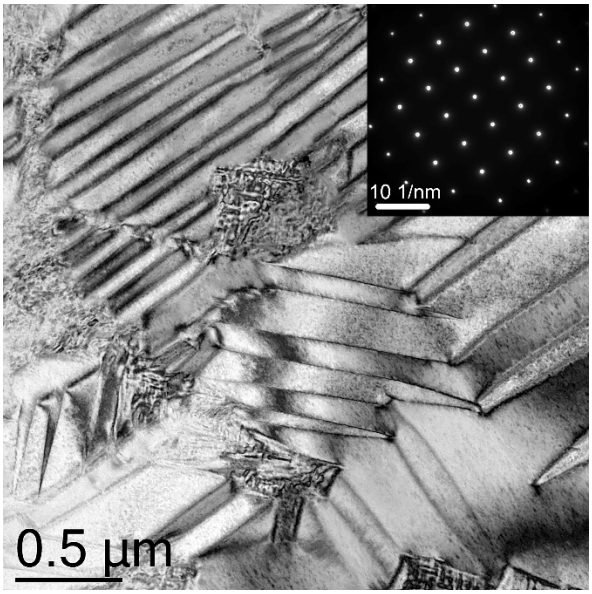

Figure 2. TEM image of 3.7Sm0.5CeSZ crystal.

The image (Figure 2) shows multiple twins. The image brightness at different sides of the twin boundary differs since lattice orientation changes upon crossing a coherent twin boundary. The twinning plane is a {110} type one. This structure is typical of all the test crystals. One can clearly see (Figure 2) two types of twin structures with different domain sizes in the crystals: a large-domain structure with typical domain sizes of 0.3–0.5 μm and a small-domain structure with typical domain sizes of < 0.1 μm located at the large-domain boundaries. Similar structures were earlier observed in the $(ZrO_2)_{1-x}(Gd_2O_3)_x$ crystals. It was shown that the regions containing large twins are the t phase whereas the smaller twins pertain to the t′ phase. The Gd_2O_3 distribution between those phases proved to be inhomogeneous [32]. One can hypothesize that the inhomogeneous composition of the tetragonal solid solutions in the test crystals also changes the morphology of their twin structure, i.e., large domains pertain to the t phase and small ones, to the t′ phase.

The microhardness data for the crystals are summarized in Table 2. It can be seen that the two-phase 3.2Sm0.5CeSZ crystals containing the monoclinic phase had the lowest microhardness. CeO_2 doping of the crystals reduced their microhardness but slightly as compared to the $(ZrO_2)_{1-x}(Sm_2O_3)_x$ crystals. The tendency of microhardness growth with Sm_2O_3 concentration observed for the $(ZrO_2)_{1-x}(Sm_2O_3)_x$ crystals is also the case for the $(ZrO_2)_{0.995-x}(Sm_2O_3)_x(CeO_2)_{0.005}$ ones.

Table 2. Microhardness of $(ZrO_2)_{1-x}(Sm_2O_3)_x$ [24] and $(ZrO_2)_{0.995-x}(Sm_2O_3)_x(CeO_2)_{0.005}$ crystals.

Composition	Microhardness, GPa	Composition	Microhardness, GPa
3.2SmSZ	10.75 ± 0.30	3.2Sm0.5CeSZ	10.54 ± 0.25
3.7SmSZ	11.30 ± 0.30	3.7Sm0.5CeSZ	11.15 ± 0.25
4.0SmSZ	12.15 ± 0.30	4.0Sm0.5CeSZ	11.70 ± 0.25

Figure 3 shows the fracture toughness of the $(ZrO_2)_{0.995-x}(Sm_2O_3)_x(CeO_2)_{0.005}$ crystals as a function of indenter diagonal orientation relative to the crystallographic directions in the specimen plane. By way of comparison, Figure 3 shows the fracture toughness of the $(ZrO_2)_{1-x}(Sm_2O_3)_x$ crystals. The data clearly suggest that CeO_2 doping in all cases increases the fracture toughness of the crystals. The relatively low fracture toughness of the 3.2Sm0.5CeSZ crystals is probably caused by the presence of the monoclinic phase. Tetragonal crystals with high fracture toughness had the most expressed anisotropy. The 3.7Sm0.5CeSZ crystals had the highest fracture toughness of 16 MPa·$m^{1/2}$.

Preprints.org (www.preprints.org) | NOT PEER-REVIEWED | Posted: 12 July 2024 doi:10.20944/preprints202407.1010.v1

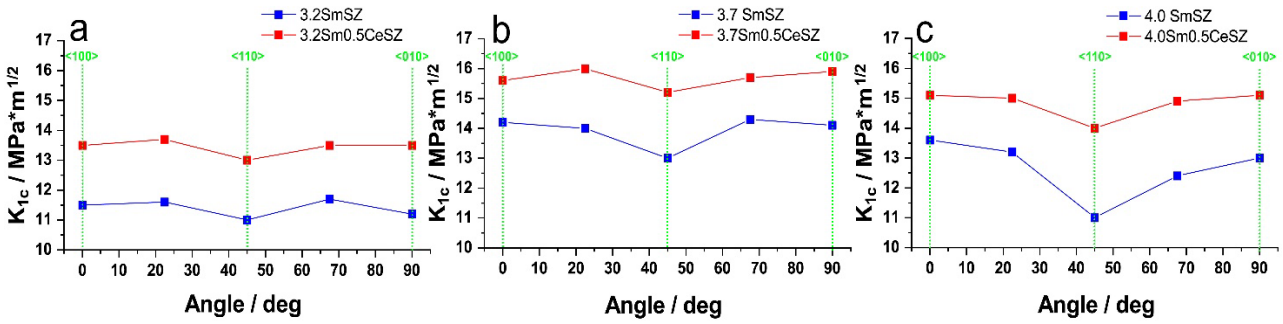

Figure 3. Fracture toughness of (a) 3.2Sm0.5CeSZ, (b) 3.7Sm0.5CeSZ and (c) 4.0Sm0.5CeSZ crystals depending on indenter diagonal orientation in {100} specimen plane. <100> direction corresponds to 0 arc deg.

It is well-known that the high fracture toughness of partially stabilized zirconia based materials originates from the transformation strengthening mechanism. Theoretical analyses of the contribution from the transformation strengthening mechanism to the fracture toughness showed that contribution to be proportional to the content of the transformable tetragonal phase, its transformability and transformation zone width [33]. Data on the transformation zone width and transformability of the tetragonal phase (Rm) (the relative quantity of the tetragonal phase that transformed to the monoclinic one) can be derived from local phase analysis around the indentation. The transformability (Rm) was calculated from the monoclinic to tetragonal phase band intensity ratio in the Raman spectra using the following formula [34]:

$$R_m = \frac{I^m_{178} + I^m_{190}}{I^t_{146} + I^m_{178} + I^m_{190}} \quad (2)$$

where Im178 and Im190 are the intensities of the 178 and 190 cm^{-1} bands in the monoclinic phase spectrum and It146 is the intensity of the 146 cm^{-1} band in the tetragonal phase spectrum. Figure 4 shows the transformation degrees at different points near the indentation for the 3.7Sm0.5CeSZ and 3.7SmSZ crystals.

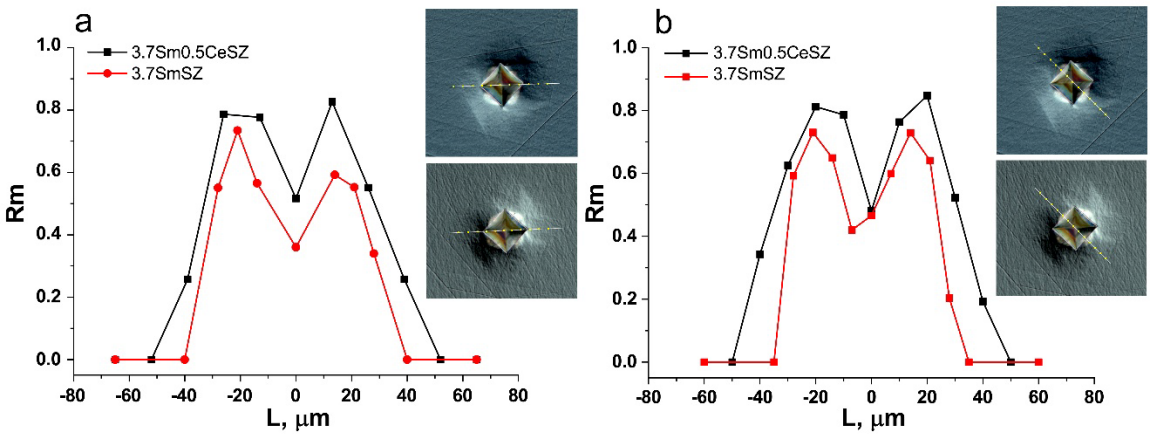

Figure 4. Degrees of tetragonal to monoclinic phase transformation for 3.7Sm0.5CeSZ and 3.7SmSZ crystals at local points near indentation for directions (a) along indenter diagonal and (b) along indenter side. Indentation boundaries are marked by dashes.

As can be seen from Figure 4, the region of the stress-induced t→m phase transition in the 3.7Sm0.5CeSZ crystals extends farther beyond the indentation boundaries than in the 3.7SmSZ crystals. The 3.7Sm0.5CeSZ crystals also exhibit a greater degree of transformation as compared to the 3.7SmSZ ones. Similar regularities were also observed for the 4.0Sm0.5CeSZ and 4.0SmSZ crystals. This indicates that the indentation stress-induced t→m phase transition in the CeO_2 doped

 doi:10.20944/preprints202407.1010.v1

crystals is more intense and covers greater regions. Both those factors increase the fracture toughness of the crystals.

Thus, analysis of the experimental data leads to the conclusion that CeO_2 doping of the $(ZrO_2)_{1-x}(Sm_2O_3)_x$ solid solutions increases the tetragonality degree of the transformable tetragonal t phase and the intensity of the indentation-induced tetragonal to monoclinic phase transition. All those factors eventually increase the fracture toughness of the CeO_2 doped $(ZrO_2)_{1-x}(Sm_2O_3)_x$ crystals.

In order to assess the high-temperature stability of the structure and mechanical properties of the crystals, we carried out air and vacuum annealing of the crystals at 1600 °C for 2 h.

Vacuum annealing changed the color of the crystals to black due to the formation of non-stoichiometric oxygen vacancies producing an intense absorption band in the visible spectrum. Annealing of the $(ZrO_2)_{0.995-x}(Sm_2O_3)_x(CeO_2)_{0.005}$ crystals regardless of composition, either in air or in vacuum, caused visible changes to their surfaces. Figure 5 shows optical surface images of the crystals upon annealing in different environments.

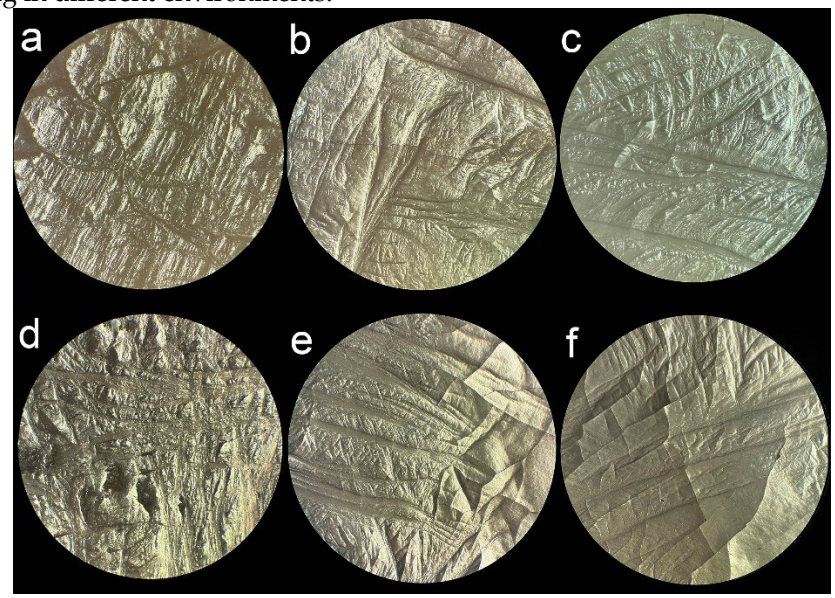

Figure 5. Surface images of (a, d) 3.2Sm0.5CeSZ, (b, e) 3.7Sm0.5CeSZ and (c, f) 4.0Sm0.5CeSZ crystals upon (a, b, c) air and (d, e, f) vacuum annealing.

The surfaces of the as-grown 3.7Sm0.5CeSZ; and 4.0Sm0.5CeSZ crystals were smooth and homogeneous. Air and vacuum annealing of those crystals produced surface roughness. The surface of the as-grown 3.2Sm0.5CeSZ crystals was inhomogeneous. Annealing of those crystals increased surface roughness and the number of microcracks. The observed changes can be caused by a change in the phase composition of the crystals upon annealing.

Thus, study of the phase composition of the CeO_2 doped crystals showed that annealing produces (or increases the quantity) of the monoclinic phase.

The observed changes in the phase composition of the crystals were accompanied by changes in their microhardness (Table 3).

Table 3. Microhardness of $(ZrO_2)_{0.995-x}(Sm_2O_3)_x(CeO_2)_{0.005}$ crystals before and after annealing in air and in vacuum.

Specimen	HV, GPa		
	As-Grown	Vacuum Annealed	Air Annealed
3.2Sm0.5CeSZ	10.54 ± 0.25	8.55 ± 0.30	8.50 ± 0.30

 doi:10.20944/preprints202407.1010.v1

3.7Sm0.5CeSZ	11.15 ± 0.25	8.65 ± 0.30	8.60 ± 0.30
4.0Sm0.5CeSZ	11.70 ± 0.25	9.25 ± 0.30	8.70 ± 0.30

All the heat-treated crystals exhibited a decrease in the microhardness, probably due to the formation or an increase in the quantity of the monoclinic phase in the crystal bulk upon annealing. Annealing environment had a negligible effect on the microhardness of the crystals.

High-temperature annealing had the greatest effect on the fracture toughness of the crystals. The as-annealed fracture toughness of the 3.2Sm0.5CeSZ, 3.7Sm0.5CeSZ and 4.0Sm0.5CeSZ crystals decreased dramatically, to within 2–3.5 MPa·$m^{1/2}$, the fracture toughness values exhibiting no anisotropy. Similar degradation of the structure and mechanical properties was earlier observed after annealing of 3.2SmSZ, 3.7SmSZ and 4.0SmSZ crystals [15].

Thus, CeO_2 doping of the $(ZrO_2)_{1-x}(Sm_2O_3)_x$ solid solutions in the experimental concentration range does not increase the high-temperature phase stability of the crystals and cannot prevent high-temperature degradation of their fracture toughness.

4. Conclusions

The effect of ceria doping of $(ZrO2)_{1-x}(Sm_2O_3)_x$ solid solutions on their phase composition, microhardness and fracture toughness was studied. Doping with 0.5 mol.% CeO_2 increases the lattice parameter c of the transformable tetragonal t phase and reduces the lattice parameter c of the non-transformable tetragonal t′ phase. The tetragonality degree of the t phase increases while that of the t′ phase decreases. CeO_2 doping causes a more profound phase separation in the (c + t) two-phase region. As a result, the composition of the transformable t phase approaches the t/(c + t) phase boundary thus making the phase more transformable, whereas the composition of the non-transformable t′ phase shifts toward the (c + t)/c phase boundary.

CeO_2 doping has but little effect on the microhardness of the crystals as compared to the $(ZrO_2)_{1-x}(Sm_2O_3)_x$ ones but increases their fracture toughness without changing the Sm2O3 concentration dependence. The 3.5Sm0.5CeSZ crystals had the highest fracture toughness,
16 MPa·$m^{1/2}$. That high fracture toughness is caused by an increase in the degree of the stress-induced tetragonal to monoclinic phase transition.

However, CeO_2 doping of the $(ZrO_2)_{1-x}(Sm_2O_3)_x$ solid solutions in the experimental concentration range did not increase the high-temperature phase stability of the crystals and did not prevent high-temperature degradation of their fracture toughness.

Author Contributions: Conceptualization, M.B., P.R., E.L. and N.T.; formal analysis, V.M., A.C., V.P, A.P., D.Z., D.K. and N.S.; investigation, N.T., N.S., A.P. and F.M.; methodology, P.R.; resources, M.B., A.K., E.L., V.M. and N.T.; supervision, M.B. and E.L.; validation, P.R. and N.T.; visualization, F.M.; writing—review and editing, M.B., N.T., E.L. and P.R. All authors have read and agreed to the published version of the manuscript.

Funding: This work was financially supported by the Moscow Polytechnic University within the framework of the grant named after Pyotr Kapitsa.

Conflicts of Interest: The authors declare no conflict of interest.

References

1. Chevalier, J.; Gremillard, L.; Virkar, A.V.; Clarke, D.R. The tetragonal-monoclinic transformation in zirconia: Lessons learned and future trends. *J. Am. Ceram. Soc.* **2009**, *92*, 1901–1920. doi.org/10.1111/j.1551-2916.2009.03278.x.
2. Hannink, R.H.J; Kelly PM; Muddle, B.C. Transformation toughening in zirconia-containing ceramics. *J. Am. Ceram. Soc.* **2000**, 83(3). doi:10.1111/j.1151-2916.2000.tb01221.x
3. Krogstad, J.A.; Krämer, S.; Lipkin, D.M.; Johnson, C.A.; Mitchell, D.R.G.; Cairney, J.M.; Levi, C.G. Phase stability of t′-zirconia-based thermal barrier coatings: Mechanistic insights. *J. Am. Ceram. Soc.* **2011**, 94(SUPPL. 1). doi:10.1111/j.1551-2916.2011.04531.x

4. Hisbergues, M; Vendeville, S; Vendeville, P. Review zirconia: *J. Biomed. Mater. Res. B Appl. Biomater*. **2009**, 88(2). doi:10.1002/jbm.b.31147
5. Deng, Y; Wang, C; Xu, X.; Li, H. Machine learning potential for Ab Initio phase transitions of zirconia. *Theoretical and Applied Mechanics Letters*. **2023**, 13(6). doi:10.1016/j.taml.2023.100481
6. Heuer, A.H. Transformation Toughening in ZrO2-Containing Ceramics. *J. Am. Ceram. Soc.* **1987,** 70(10). doi:10.1111/j.1151-2916.1987.tb04865.x
7. Lorenzo-Martin, C; Ajay, O.O; Singh, D; Routbort, J.L. Evaluation of scuffing behavior of single-crystal zirconia ceramic materials. *Wear*. **2007**, 263(7-12 SPEC. ISS.). doi:10.1016/j.wear.2006.12.054
8. Cheng, J; Tian, C; Yang, J; He, J. Electrical and mechanical properties of Sm2O3 doped Y-TZP electrolyte ceramics. *Ceram Int*. **2018**, 44(14). doi:10.1016/j.ceramint.2018.06.146
9. Bejugama, S; Chameettachal, S; Pati, F;. Pandey, A.K. Tribology and in-vitro biological characterization of samaria doped ceria stabilized zirconia ceramics. *Ceram Int*. **2021**, 47(12). doi:10.1016/j.ceramint.2021.03.076
10. Grathwohl, G; Liu, T. Crack Resistance and Fatigue of Transforming Ceramics: II, CeO2-Stabilized Tetragonal ZrO2. *J. Am. Ceram. Soc.* **1991**, 74(12). doi:10.1111/j.1151-2916.1991.tb04297.x
11. Rauchs, G; Fett, T; Munz, D; Oberacker R. Tetragonal-to-monoclinic phase transformation in CeO2-stabilised zirconia under uniaxial loading. *J. Eur. Ceram. Soc*. **2001**, 21(12). doi:10.1016/S0955-2219(00)00258-2
12. Palmero, P; Fornabaio, M; Montanaro, L; Reveron, H.; Esnouf, C.; Chevalier, J. Towards long lasting zirconia-based composites for dental implants: Part I: Innovative synthesis, microstructural characterization and invitro stability. *Biomaterials*. **2015**, 50(1). doi:10.1016/j.biomaterials.2015.01.018
13. Savin, A; Craus, M.L; Turchenko, V; Bruma, A.; Dubos, P.A.; Malo, S; Konstantinova, T.E.; Burkhovetsky, V.V. Monitoring techniques of cerium stabilized zirconia for medical prosthesis. *Applied Sciences*. **2015**, 5(4). doi:10.3390/app5041665
14. Reveron, H; Fornabaio, M; Palmero, P; Fürderer, T.; Adolfsson, E.; Lughi, V.; Bonifacio, A.; Sergo, V.; Montanaro, L.; Chevalier, J. Towards long lasting zirconia-based composites for dental implants: Transformation induced plasticity and its consequence on ceramic reliability. *Acta Biomater*. **2017**, 48. doi:10.1016/j.actbio.2016.11.040
15. Borik, M.A; Kulebyakin, A.V.; Lomonova, E.E; Milovich, F.O.; Myzina, V.A.; Ryabochkina, P.A.; Sidorova, N.V.; Tabachkova, N.Yu.; Chislov A.S. Effect of heat treatment on the structure and mechanical properties of zirconia crystals partially stabilized with samarium oxide. *Modern Electronic Materials*. **2023**, 9(3). doi:10.3897/j.moem.9.3.115614
16. Kisi, E.H; Howard, C.J. Crystal structures of zirconia phases and their inter-relation. *Key. Eng. Mater*. **1998**, (153-154). doi:10.4028/www.scientific.net/kem.153-154.1
17. Guo, L; Li, M; Zhang, C; Huang, X; Ye, F. Dy2O3 stabilized ZrO2 as a toughening agent for Gd2Zr2O7 ceramic. *Mater. Lett*. **2017**, 188. doi:10.1016/j.matlet.2016.11.038
18. Zhu, W; Nakashima, S; Marin, E; Gu H.; Pezzotti, G. Annealing-induced off-stoichiometric and structural alterations in ca^{2+} - and y^{3+} - stabilized zirconia ceramics. *Materials*. **2021**, 14(19). doi:10.3390/ma14195555
19. Schulz, U. Phase transformation in EB-PVD yttria partially stabilized zirconia thermal barrier coatings during annealing. *J. Am. Ceram. Soc.* **2000**, 83(4). doi:10.1111/j.1151-2916.2000.tb01292.x
20. Zhu, W.; Fujiwara, A.; Nishiike, N.; Nakashima, S.; Gu, H.; Marin, E.; Sugano, N.; Pezzotti, G. Mechanisms induced by transition metal contaminants and their effect on the hydrothermal stability of zirconia-containing bioceramics: An XPS study. *Phys. Chem. Chem. Phys*. **2018**, 20(45). doi:10.1039/c8cp06027d
21. Zhu, W; Nakashima, S; Marin, E; Gu, H.; Pezzotti, G. Microscopic mapping of dopant content and its link to the structural and thermal stability of yttria-stabilized zirconia polycrystals. *J. Mater. Sci*. **2020**, 55(2). doi:10.1007/s10853-019-04080-9
22. Turon-Vinas, M; Roa, J.J; Marro, F.G; Anglada, M. Mechanical properties of 12Ce-ZrO2/3Y-ZrO2 composites. *Ceram. Int*. 2015;41(10). doi:10.1016/j.ceramint.2015.08.044
23. Borik, M; Kulebyakin V; Myzina V; Lomonova, E.E.; Milovich, F.O.; Ryabochkina P.A.; Sidorova, N.V.; Shulga, N.Y.; Tabachkova, N.Y. Mechanical characteristics, structure, and phase stability of tetragonal crystals of ZrO2–Y2O3 solid solutions doped with cerium and neodymium oxides. *J. Phys. Chem. Solids.* 2021;150. doi:10.1016/j.jpcs.2020.109808
24. Borik, M; Chislov, A; Kulebyakin, A; Lomonova, E.E.; Milovich, F.O.; Myzina V; Ryabochkina P.A.; Sidorova, N.V.; Tabachkova, N.Y. Phase Composition and Mechanical Properties of Sm_2O_3 Partially Stabilized Zirconia Crystals. *Crystals*. **2022**, 12(11). doi:10.3390/cryst12111630
25. Niihara, K. A fracture mechanics analysis of indentation-induced Palmqvist crack in ceramics. *J. Mater. Sci. Lett*. **1983**, 2(5). doi:10.1007/BF00725625
26. Niihara, K; Morena R; Hasselman D.P.H. Evaluation of KIc of brittle solids by the indentation method with low crack-to-indent ratios. *J. Mater. Sci. Lett*. **1982**, 1(1). doi:10.1007/BF00724706

27. Moradkhani, A; Baharvandi, H. Effects of additive amount, testing method, fabrication process and sintering temperature on the mechanical properties of Al2O3/3Y-TZP composites. *Eng. Fract. Mech.* **2018**, 191. doi:10.1016/j.engfracmech.2017.12.033
28. Orera, V.M; Merino, R.I; Peña, F. $Ce^{3+}\leftrightarrow Ce^{4+}$ conversion in ceria-doped zirconia single crystals induced by oxido-reduction treatments. *Solid State Ion.* **1994**, 72(PART 2). doi:10.1016/0167-2738(94)90151-1
29. Kozlova, A.P; Kasimova, V.M; Buzanov, O.A; Chernenko, K.; Klementiev, K.; Pankratov, V. Luminescence and vacuum ultraviolet excitation spectroscopy of cerium doped $Gd_3Ga_3Al_2O_{12}$ single crystalline scintillators under synchrotron radiation excitations. *Results Phys.* **2020**, 16. doi:10.1016/j.rinp.2020.103002
30. Yoshimura, M; Yashima, M; Noma, T; Sōmiya, S. Formation of diffusionlessly transformed tetragonal phases by rapid quenching of melts in ZrO 2 -RO 1.5 systems (R = rare earths). *J. Mater. Sci.* **1990**, 25(4). doi:10.1007/BF01045757
31. Kern, F. Ytterbia-neodymia-costabilized TZP-Breaking the limits of strength-toughness correlations for zirconia? *J. Eur. Ceram. Soc.* **2013**, 33(5). doi:10.1016/j.jeurceramsoc.2012.10.028
32. Borik, M.A.; Chislov, A.S.; Kulebyakin, A.V.; Lomonova, E.E.; Milovich, F.O.; Myzina, V.A.; Ryabochkina, P.A.; Sidorova, N.V.; Tabachkova, N.Y. Effect of heat treatment on the structure and mechanical properties of partially gadolinia-stabilized zirconia crystals. *J. Asian Ceram. Soc.* **2021**, *9*, 559–569. https://doi.org/10.1080/21870764.2021.1903150.
33. Evans, A.G; Cannon, R.M. Overview no. 48. Toughening of brittle solids by martensitic transformations. *Acta Metallurgica.* **1986**, 34(5). doi:10.1016/0001-6160(86)90052-0
34. Chien, F.R; Ubic, F.J; Prakash; V, Heuer, A.H. Stress-induced martensitic transformation and ferroelastic deformation adjacent microhardness indents in tetragonal zirconia single crystals. *Acta Mater.* **1998**, 46(6). doi:10.1016/S1359-6454(97)00444-8